

EVOLUTION OF LYMAN-LIMIT ABSORPTION SYSTEMS OVER THE REDSHIFT RANGE $0.40 < z < 4.69$

L. J. STORRIE-LOMBARDI AND R. G. MCMAHON

Institute of Astronomy, Madingley Road, Cambridge CB3 0HA, UK

M. J. IRWIN

Royal Greenwich Observatory, Madingley Road, Cambridge CB3 0EZ, UK

AND

C. HAZARD

University of Pittsburgh, Pittsburgh, PA 15260; and Institute of Astronomy

Received 1993 October 28; accepted 1994 March 4

ABSTRACT

We present the results of a study of 15 $z > 4.2$ QSOs that extend statistical studies of Lyman-limit absorption line systems [$N(\text{H I}) \geq 1.6 \times 10^{17} \text{ cm}^{-2}$] to the highest redshifts currently possible. This data set has been combined with homogeneous data sets of low-redshift *Hubble Space Telescope* observations and intermediate-redshift ground-based observations.

Assuming a power law of the form $N(z) = N_0(1+z)^\gamma$ for the number density, we find $\gamma = 1.55$ and $N_0 = 0.27$, with $N = 3.27$ per unit redshift at $z = 4$. The $>99.7\%$ confidence limits for γ are 2.37 and 0.82. For the first time this indicates intrinsic evolution of these absorbers for an $\Omega = 1$ universe ($\gamma = \frac{1}{2}$ for no evolution). This result is marginally consistent with no evolution for $\Omega = 0$ ($\gamma = 1$ for no evolution). These results differ significantly from those of Sargent, Steidel, & Boksenberg (1989) who found no intrinsic evolution in Lyman-limit systems up to $z = 3.5$, and Lanzetta (1991) who found much stronger evolution for $z > 2.5$.

For $z \lesssim 2$ the space density of Lyman limit systems [$N(1.5) \approx 1.1$] and Mg II absorbers with rest equivalent width $W_0 > 0.3 \text{ \AA}$ [$N(1.5) \approx 1.0$] is almost identical. This supports the picture that Lyman-limit and Mg II absorbers are drawn from the same population.

Subject headings: galaxies: evolution — quasars: absorption lines

1. INTRODUCTION

Lyman-limit systems (LLS) are defined and detected by the observation of neutral hydrogen (H I) absorption which is optically thick to Lyman-continuum radiation for $\lambda < 912 \text{ \AA}$, the Lyman limit, corresponding to a column density $N(\text{H I}) \geq 1.6 \times 10^{17} \text{ cm}^{-2}$. They are easily identified in the optical spectra of high-redshift QSOs by a sharp drop in the continuum flux shortward of $\lambda = 912 \text{ \AA}$ in the rest frame of the absorbers. Unlike the more numerous Ly α forest lines, LLS are always observed to have associated metal lines (e.g., C IV and S II) (Steidel 1990) and are thought to originate in galactic disks and halos or in galaxy progenitors. Observational support for this view comes from the work of Bergeron & Boisse (1991) who have shown Mg II absorption to be associated with the extended halos of bright galaxies. Much work supports the hypothesis that LLS are the parent population from which Mg II absorbers are drawn for $z \lesssim 2$ (Bergeron & Stasinska 1986; Lanzetta, Turnshek, & Wolfe 1987; Steidel & Sargent 1992; and references therein). Bergeron & Stasinska showed that the observed average ionization level of the absorbing clouds depends crucially on H I column density, with the critical value at $N(\text{H I}) \sim 10^{17-18} \text{ cm}^{-2}$. The Mg II absorbers all had column densities above this threshold. Many more Mg II absorption systems are known than LLS since from the ground Mg II absorption can be observed over the redshift range $0.2 \leq z \leq 2.2$ while LLS can only be detected for $z \gtrsim 2.5$.

Since LLS completely absorb UV radiation shortward of 912 \AA in the QSO rest frame, their number density is a key

factor in determining the origin of the UV background ionizing flux (Zuo & Phinney 1993). The space density of LLS not only determines the mean free path of the ionizing UV photons but hardens the radiation as well since the absorption cross section for H I varies as $\sim \lambda^3$ for $\lambda < 912 \text{ \AA}$ [i.e., $\tau_{\lambda < 912} = \tau_{912}(\lambda/\lambda_{912})^3$] (Osterbrock 1989). Attempts to explain the UV background by QSOs or star-forming protogalaxies must therefore include the effect of intervening Lyman-limit absorbers.

The statistical properties of LLS were first studied by Tytler (1982) using a heterogeneous data set of ground-based and *International Ultraviolet Explorer (IUE)* observations. He showed that they were a cosmologically intervening population and found no evidence for significant intrinsic evolution in the absorbers for $0.4 < z < 3.5$. More recent work disagrees in the form of the evolution observed. Sargent, Steidel, & Boksenberg (1989, hereafter SSB), detected no intrinsic evolution in the absorbers up to $z \sim 4$. Lanzetta (1991) also found no evolution for $z < 2.5$ but detected strong evolution for $z > 3$, toward the high-redshift limit of his data set.

The recent discovery (Irwin, McMahon, & Hazard 1991) of substantial numbers of $z > 4$ QSOs which are bright enough for absorption-line studies enables for the first time detailed studies of QSO absorption lines at redshifts greater than 4. At $z > 4$ the age of the universe ($\sim 10^9$ yr) is comparable with the collapse timescale for protogalaxies so that observational information on this epoch is a direct constraint on theories of galaxy formation (e.g., Fall & Rees 1985; Rees 1988).

We extend studies of Lyman-limit system evolution to $z > 4$

using new observations of 15 bright, $z \geq 4.2$ QSOs ($4.20 \leq z_{\text{em}} \leq 4.69$). These are combined with ground-based optical observations of 53 intermediate-redshift QSOs ($2.75 < z_{\text{em}} < 4.11$) by SSB and *Hubble Space Telescope* (*HST*) UV observations of 29 low-redshift QSOs ($0.47 < z_{\text{em}} < 1.40$) (Bahcall et al. 1993). In a companion paper (Williger et al. 1994) we present a study of the Ly α forest lines in the spectrum of the $z = 4.5$ QSO BRI 1033–0327.

2. OBSERVATION AND SAMPLE SELECTION

2.1. New High-Redshift Observations

The observations were carried out with the William Herschel Telescope on La Palma in 1992 April and October and 1993 April and August using the ISIS spectrograph with 158 line mm^{-1} gratings at 5 Å resolution. In the red arm we used an EEV detector with 22.5μ pixels ($2.71 \text{ Å pixel}^{-1}$) covering 5500–8800 Å. In the blue arm we used a thinned TEK1024 detector with 24μ pixels ($2.89 \text{ Å pixel}^{-1}$) covering 3200–6000 Å. A 5400 Å dichroic enabled red and blue arm observations to be carried out simultaneously. For this program we observed 14 non-BAL, $z \geq 4.2$ QSOs from the APM Multicolor Survey for bright ($m_r < 19$) $z > 4$ QSOs and one $z = 4.3$ radio-selected QSO (GB 1508+5714) from Hook et al. (1994). The broad absorption line (BAL) QSOs were excluded since they are a class of QSO which shows broad (up to $\sim 30,000 \text{ km s}^{-1}$) absorption from predominantly highly ionized species, e.g., S IV, C IV, and O VI, which is believed to be intrinsic to the QSO (e.g., Hazard et al. 1984). Due to this absorption, the spectrum shortward of $\sim 1000 \text{ Å}$ in the rest frame is unsuitable for Lyman-limit system studies.

To minimize any possible color selection bias, only APM QSOs with $z_{\text{em}} \geq 4.2$ are included in this study. By this redshift the average intervening cosmological absorption due to the Ly α forest alone is sufficient to make the color of the QSOs red enough in $B_r - R$ to drive them well away from the main stellar locus (Irwin, McMahon, & Hazard 1991).

Lyman-limit systems were clearly visible in the spectra of all of the QSOs. The absorption redshifts were initially determined interactively by examining the spectral region around the discontinuity and finding the wavelength where the continuum reached a minimum. The visual identifications were compared with an automated detection algorithm in which the redshift was determined from the wavelength λ_f where the median flux ratio (f) in bins 50 Å wide (rest frame) shortward and longward of λ_f reached a minimum. The agreement with the visual determinations was excellent, with the mean $\Delta z = 0.011 \pm 0.017$. The optical depth at the Lyman limit, $\tau_{\text{lls}} = -\ln(f)$, was estimated using the median flux in bins 50 Å wide in the rest frame of the absorber on either side of the break. Hereafter we use the automated determinations. If more than one LLS was detected, only the highest redshift LLS with $\tau > 1$ was included in the sample. The high-redshift observations are summarized in Table 1. The spectra of the $z > 4.2$ QSOs utilized in this Letter are available via anonymous ftp from ftp.ast.cam.ac.uk in the compressed postscript file pub/apm/apm_lls.ps.Z. They will be published in Storrie-Lombardi et al. (1994).

2.2. The Statistical Sample

In three of the 15 $z > 4.2$ QSOs (BR 0245–0608, BRI 1114–0822, BRI 1335–0417) and three of the 53 observations published in Table 6 of SSB (Q0004+171, Q0054–284, Q1836+511), LLS are detected within 4000 km s^{-1} of the

TABLE 1
HIGH-REDSHIFT OBSERVATIONS

QSO	Date ^a	Exp (s)	z_{em}^b	z_{min}^c	z_{lls}^d	τ_{lls}^e
BR 0019–1522	3	2700	4.52	2.51	4.27	> 5.8
BR 0103+0032 ^f	6	3000	4.44	2.51	4.31	1.6
					4.15	> 1.6
BRI 0151–0025	6	3000	4.20	2.51	4.05	> 3.7
BR 0245–0608 ^g	6	3000	4.24	2.51	4.23	> 3.9
BR 0951–0450	2	2700	4.37	2.84	4.22	> 3.1
BRI 0952–0115	1, 2	3400	4.43	2.84	4.25	> 2.1
BRI 1013+0033	2	2700	4.41	2.84	3.78	> 2.3
BR 1033–0327	5	3000	4.51	2.84	4.19	> 3.5
BRI 1050–0000	2	1800	4.29	2.84	4.08	> 2.5
BRI 1114–0822 ^g	4	2700	4.51	2.84	4.50	> 3.7
BR 1202–0725	5	2700	4.69	2.84	4.52	> 3.0
BRI 1328–0433 ^f	5	2700	4.22	2.84	4.25	0.6
					3.31	> 1.5
BRI 1335–0417 ^g	2	2700	4.40	2.84	4.45	> 3.1
GB 1508+5714	5	2700	4.30	2.84	3.88	> 4.6
BR 2237–0607	3	2700	4.56	2.51	4.28	> 2.6

^a Date code: (1) 1992 Apr 6, (2) 1992 Apr 24/25, (3) 1992 Oct 3/4, (4) 1993 Apr 11, (5) 1993 Apr 17, and (6) 1993 Aug 21.

^b z_{em} = QSO emission redshift.

^c z_{min} = minimum redshift at which a LLS could be observed.

^d z_{lls} = LLS redshift.

^e τ_{lls} = optical depth at the Lyman-limit.

^f The highest z , $\tau > 1$, LLS is counted in the sample.

^g $[(z_{\text{em}} - z_{\text{lls}})/(1 + z_{\text{em}})] \times c < 4000 \text{ km s}^{-1}$.

QSO emission redshift. These may not be typical intervening systems since they could be affected by the UV radiation from the QSO or they could be associated with the QSO, i.e., intrinsic to the host galaxy or clustered with the QSO. In addition, uncertainties exist in the systemic QSO emission redshifts in that redshifts determined from high- and low-ionization lines exhibit differences up to 2000 km s^{-1} (e.g., Steidel & Sargent 1991). Results are presented with and without the six objects with absorbers within 4000 km s^{-1} of z_{em} . At $z > 4$, Ly α and C IV are the only strong emission lines visible but Ly α is almost 50% absorbed by the Ly α forest, making it difficult to use for redshift determination. The QSO redshifts were determined from the mean z of the O I + S II, Si IV + O IV, and C IV emission lines. Q0302+171 from SSB exhibits BAL characteristics and was removed from the sample. All 29 *HST* observations reported in Table 10 of Bahcall et al. (1993) are included but z_{lls} was determined using our automated detection algorithm. The published redshifts agree well ($z_{\text{lls}} - z_{\text{published}} = -0.009 \pm 0.016$), but we measure $\tau_{\text{lls}} > 1.0$ for seven absorbers as opposed to five in the published data. We have measured the optical depths interactively as our automated measurement algorithm underestimates τ_{lls} due to background subtraction problems in some of the *HST* spectra. The *HST* Lyman limit systems are summarized in Table 2.

TABLE 2
HST LYMAN-LIMIT SYSTEMS WITH $\tau > 1.0$

QSO	z_{em}	z_{min}	z_{lls}	τ_{lls}
Q1022+1927 (4C 19.34)	0.828	0.404	0.546	1.42
Q1038+0625 (4C 06.41)	1.270	0.404	0.456	1.15
PKS 1055+2007	1.110	0.404	1.036	2.68
Q1317+2743 (Ton 153)	1.022	0.404	0.649	4.43
PG 1352+0106	1.121	0.404	0.677	6.70
PKS 1354+1919	0.720	0.404	0.470	1.70
PKS 1424–1150	0.805	0.404	0.666	2.20

Excluding the six QSOs with $z_{\text{lls}} < 4000 \text{ km s}^{-1}$ from z_{em} gives a final statistical sample of 90 QSOs spanning $0.47 < z_{\text{em}} \leq 4.69$ and 48 LLS covering $0.45 < z_{\text{lls}} \leq 4.52$. Including the former six QSOs, the sample covers the same redshift ranges.

3. ANALYSIS

We examine the redshift evolution of the Lyman-limit systems by determining the number density of absorbers per unit redshift, $dN/dz \equiv N(z)$. In a standard Friedmann universe for absorbers with cross section πR_0^2 and number density Φ_0 per unit comoving volume,

$$N(z) = \Phi_0 \pi R_0^2 c H_0^{-1} (1+z)(1+2q_0 z)^{-1/2}.$$

It is customary to represent the number density as a power law of the form

$$N(z) = N_0 (1+z)^\gamma,$$

where $N_0 = \Phi_0 \pi R_0^2 c H_0^{-1}$. For no evolution of the absorber population this yields $\gamma = 1$ for $q_0 = 0$ and $\gamma = \frac{1}{2}$ for $q_0 = \frac{1}{2}$.

We obtained maximum likelihood estimates using unbinned data for γ and N_0 simultaneously. The log-likelihood function with $>68.3\%$, $>95.5\%$, and $>99.7\%$ confidence contours is plotted in Figure 1 for the data set excluding the absorbers within 4000 km s^{-1} of z_{em} . The most likely values for γ and N_0 yield $N(z) = 0.27_{-0.13}^{+0.20} (1+z)^{1.55 \pm 0.45}$, with $N = 3.27$ at $z = 4$. The $>99.7\%$ confidence limits for γ are 2.37 and 0.82. For the first time this indicates intrinsic evolution of these absorbers assuming a single power-law form for the redshift evolution, for an $\Omega = 1$ universe. This result is marginally consistent with no evolution for $\Omega = 0$. Including all the absorbers in the analysis yields $N(z) = 0.25_{-0.11}^{+0.19} (1+z)^{1.53 \pm 0.42}$ with $>99.7\%$ confidence limits for γ of 2.30 and 0.84. A Kolmogorov-Smirnov (K-S) test gives probabilities of 0.29 and 0.70 for the fits when the absorbers within 4000 km s^{-1} are excluded and included, respectively. The single power law represents the underlying distribution well in both cases. If two power-law models are fitted to the data we find for $z < 3$, $N_0 = 0.38_{-0.18}^{+0.31}$ and $\gamma = 1.04 \pm 0.59$, and for $z > 2.5$, $N_0 = 0.043_{-0.03}^{+0.2}$ and $\gamma = 2.8_{-1.1}^{+0.9}$, yielding a K-S probability of 0.82. A double power law does not fit the underlying distribution significantly better than a single power law. These results are summarized in Table 3.

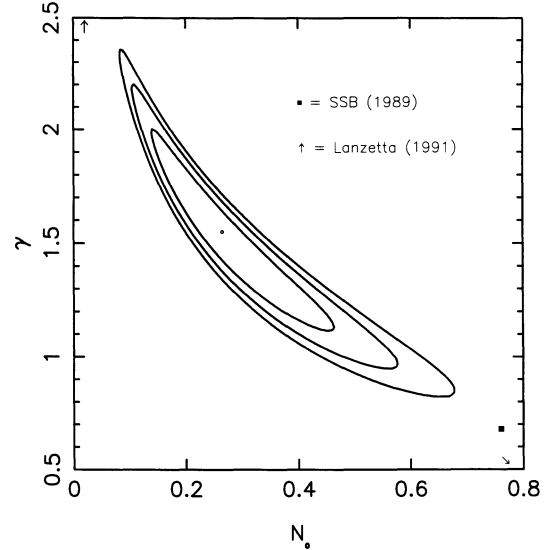


FIG. 1.—The log-likelihood function with peak at $\gamma = 1.55$, $N_0 = 0.27$, and $>68.3\%$, $>95.5\%$, and $>99.7\%$ confidence contours. The results for SSB and Lanzetta (1991) are shown using the values quoted in Table 3 by the filled box and arrows, respectively.

These data are customarily displayed as $dN(z)/dz$ versus $z_{\text{absorption}}$. Figure 2 shows the data with the vertical error bars placed at the mean redshift in each bin. The $N(z) = 0.27(1+z)^{1.55}$ fit is the solid line and the $z > 2.5$ portion of the two power-law fit is the dash-dot-dash line. The SSB and Lanzetta results are overplotted as dashed and dotted lines, respectively, using the values quoted in Table 3.

An alternative method of displaying the data which is not prone to the subjectivity of binning is shown in Figure 3. This shows the cumulative number of absorbers in a stepwise plot versus $z_{\text{absorption}}$. Overplotted is the expected number of LLS at each absorption redshift, i.e., $\sum_{i=1}^n \int_{z_{\text{min}}^i}^{z_{\text{max}}^i} 0.27(1+z)^{1.55} dz$. In QSOs with no LLS, z_{min} is the lowest redshift at which one could have been observed. In QSOs with an absorber, $z_{\text{min}} = z_{\text{lls}}$. If the QSOs with a LLS within 4000 km s^{-1} are excluded, $z_{\text{max}} = z_{\text{max}} - 4000 \text{ km s}^{-1}$. Otherwise, $z_{\text{max}} = z_{\text{em}}$.

TABLE 3

SUMMARY OF γ AND N_0 FOR $N(z) = N_0(1+z)^\gamma$

Sample	Redshift Range	γ	N_0	K-S Probability
This paper	0.40–4.69	1.55 ± 0.45	$0.27_{-0.13}^{+0.20}$	0.29
		0.82, 2.37 ^a	$0.27, 0.60^a$	
		1.53 ± 0.42^b	0.25^b	0.70 ^b
	<3.0	$0.84, 2.30^{a,b}$	$0.09, 0.63^{a,b}$	
		1.04 ± 0.59	$0.38_{-0.18}^{+0.31}$	0.82 ^c
	>2.5	$0.05, 2.10^a$	$0.10, 1.08^a$	
SSB 1989	0.67–4.11	0.68 ± 0.54	0.76	1.6×10^{-2}
Lanzetta 1991	0.36–2.50	0.3 ± 0.9	1.2	$< 10^{-5}$
	2.50–4.11	5.7 ± 1.9	8.1×10^{-4}	

^a $>99.7\%$ confidence limits.

^b Including $(z_{\text{em}} - z_{\text{lls}}) < 4000 \text{ km s}^{-1}$.

^c When combined with fit for $z > 2.5$.

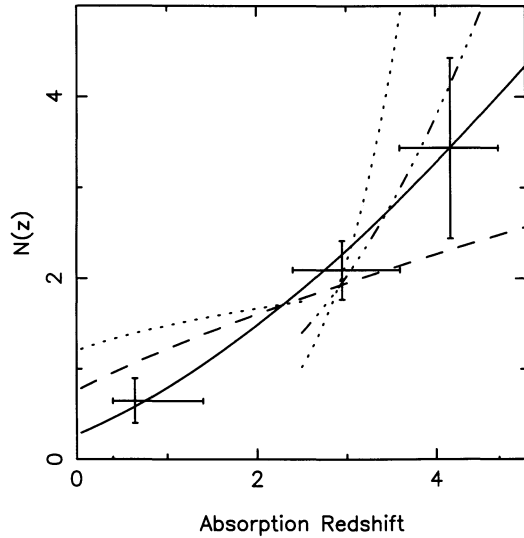


FIG. 2.—Binned distribution of the number density of LLSs per unit redshift, $N(z)$, vs. the absorption redshift. Plotted as a solid line over the entire redshift range is $N(z) = 0.27(1+z)^{1.55}$. These results exclude the QSOs with absorbers within 4000 km s^{-1} of z_{em} . The $z > 2.5$ portion of the two power-law fit is shown by a dash-dot-dash line. The SSB and Lanzetta results for $N(z)$ are overplotted as dashed and dotted lines, respectively, using the values quoted in Table 3.

4. SUMMARY AND DISCUSSION

A K-S test yields a probability of 1.6×10^{-2} when the SSB fit [$N(z) = 0.76(1+z)^{0.68}$] is applied to our data set. Our results differ for two reasons. First, the new $z > 4.2$ observations extend the absorption redshift range from $z_{\text{lls}} = 3.58$ to 4.52. Second, the new *HST* low-redshift data set (Bahcall et al. 1993) yields a lower number density than the *IUE* data used in previous studies, increasing γ .

Our analysis does not support the strong evolution detected in the data set used by Lanzetta (1991). The K-S probability is $\ll 10^{-5}$ when Lanzetta's fit is applied to the data set utilized in this Letter. While Lanzetta found that his data set was “well fitted” visually by a double power law with $\gamma = 0.3 \pm 0.9$ for $z_{\text{lls}} < 2.5$ and $\gamma = 5.7 \pm 1.9$ for $z_{\text{lls}} \geq 2.5$, the double power law does not necessarily provide a better fit in a statistical sense than a single power law. Lanzetta's sample includes 24 of 147 $z > 2.5$ QSOs with either z_{lls} or z_{min} less than 4000 km s^{-1} from z_{em} . Moreover, in at least two of the highest redshift QSOs in the Lanzetta sample, the color selected $z = 3.616$ QSO DHM 0053–2824 and the objective prism selected $z = 3.554$ QSO HM 2239–3836, the presence of the LLS contributed to their discovery. Both of these factors increase γ at high redshift. The higher space density determined from the heterogeneous *IUE* data set results in a lower γ at low redshift. In combination,

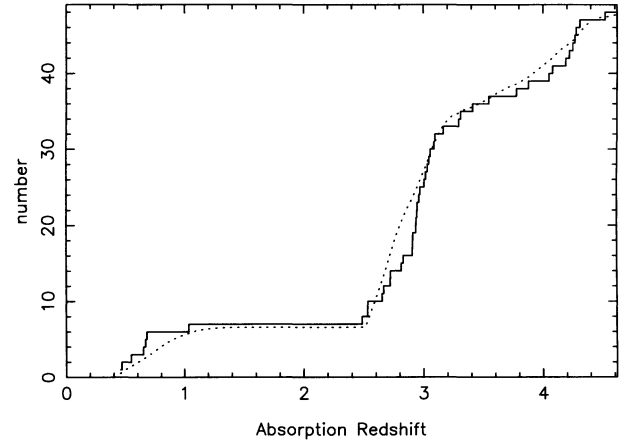


FIG. 3.—The number of Lyman-limit systems detected vs. the absorption redshift. Overplotted is $\sum_{i=1}^n \int_{z_{\text{min}}^i}^{z_{\text{max}}^i} 0.27(1+z)^{1.55} dz$.

these may explain the sharp break in the two power-law fit found for the Lanzetta (1991) data.

It has been proposed that LLS and Mg II absorbers are drawn from the same population. For $z \lesssim 2$ we find the space density for LLS [$N(1.5) \approx 1.1$] is consistent with that obtained for Mg II systems with rest equivalent width $W_0 > 0.30 \text{ \AA}$ [$N(1.5) \approx 1.0$] (Steidel & Sargent 1992). They found $\gamma = 0.78 \pm 0.42$ for the Mg II absorbers, agreeing with the SSB results of $\gamma = 0.68 \pm 0.54$ for LLSs, but the space density for the Mg II absorbers was consistently lower than for the LLSs [$N(1.5) \approx 1.4$]. They suggested this might be due to $\approx 20\%$ of the Mg II absorbers falling below the sample threshold of $W_0 = 0.30$, however given the high S/N of many of the spectra these lower equivalent width systems should have been detected and are probably quite rare (Steidel & Sargent 1992; Steidel 1993). The similarity of the space density we measure for LLS and Steidel & Sargent measure for Mg II absorbers for $z \sim 2$ supports the argument that these are drawn from the same population. The evolution of Mg II is well determined for $z < 2$ based on ~ 100 systems. Future *HST* observations should improve the statistics for LLS with $1.5 < z < 2.5$. It will be important to see if the rate of Lyman-limit evolution over this redshift range decreases since this would imply a steepening of γ toward higher redshifts. These results are based on observations obtained with the William Herschel Telescope operated on the island of La Palma by the Royal Greenwich Observatory in the Spanish Observatorio del Roque de los Muchachos of the Instituto de Astrofísica de Canarias.

We would like to thank Max Pettini and the referee for helpful suggestions. L. S. L. acknowledges support from an Isaac Newton Studentship and the Cambridge Overseas Trust. R. G. M. acknowledges the support of the Royal Society.

REFERENCES

- Bahcall, J. N., et al. 1993, *ApJS*, 87, 1
 Bergeron, J., & Boisse, P. 1991, *A&A*, 243, 344
 Bergeron, J., & Stasinska, G. 1986, *A&A*, 169, 1
 Fall, S. M., & Rees, M. J. 1985, *ApJ*, 298, 18
 Hazard, C., Morton, C. C., Terlevich, R., & McMahon, R. G. 1984, *ApJ*, 282, 33
 Hook, I. M., et al. 1994, *MNRAS*, submitted
 Irwin, M. J., McMahon, R. G., & Hazard, C. 1991, in *The Space Distribution of Quasars* (ASP Conf. Ser., 21), 117
 Lanzetta, K. M. 1991, *ApJ*, 375, 1
 Lanzetta, K. M., Turnshek, D. A., & Wolfe, A. M. 1987, *ApJ*, 322, 739
 Osterbrock, D. E. 1989, *Astrophysics of Gaseous Nebulae and Active Galactic Nuclei* (Mill Valley, CA: University Science Books), 14
 Rees, M. J. 1988, *MNRAS*, 231, 91P
 Sargent, W. L. W., Steidel, C. C., & Boksenberg, A. 1989, *ApJS*, 79, 703 (SSB)
 Steidel, C. C. 1990, *ApJS*, 74, 37
 ———. 1993, in *Proc. of the Third Teton Summer Astrophysics Conference*, ed. J. Shull & H. Thronson (Dordrecht: Kluwer), in press
 Steidel, C. C., & Sargent, W. L. W. 1991, *ApJ*, 382, 433
 ———. 1992, *ApJS*, 80, 1
 Storrie-Lombardi, L. J., et al. 1994, in preparation
 Tytler, D. 1982 *Nature*, 298, 427
 Williger, G. M., Baldwin, J. A., Carswell, R. F., Cooke, A. J., Hazard, C., Irwin, M. J., McMahon, R. G., & Storrie-Lombardi, L. J. 1994, *ApJ*, in press
 Zuo, L., & Phinney, E. S. 1993, *ApJ*, 418, 28